GEOPHYSICS, VOL. 67, NO. 2 (MARCH-APRIL 2002); P. 448–458, 9 FIGS.
10.1190/1.1468604

Atmospheric sources for audio-magnetotelluric (AMT) sounding

Xavier Garcia* and Alan G. Jones‡

ABSTRACT

The energy sources for natural-source magnetotelluric (MT) frequencies >1 Hz are electromagnetic (EM) waves caused by distant lightning storms and which propagate within the Earth–ionosphere waveguide. The properties of this waveguide display diurnal, seasonal, and 11-year solar-cycle fluctuations, and these temporal fluctuations cause significant signal amplitude attenuation variations—especially at frequencies in the 1- to 5-kHz so-called audiomagnetotelluric (AMT) dead band. In the northern hemisphere these variations increase in amplitude during the nighttime and the summer months, and they correspondingly decrease during the daytime and the winter months. Thus, one problem associated with applying the AMT method for shallow (<3 km) exploration can be the lack of signal in certain frequency bands during the desired acquisition interval. In this paper we analyze the time variations of high-frequency EM fields to assess the limitations of the efficient applicability of the AMT method. We demonstrate that magnetic field sensors need to become two orders of magnitude more sensitive than they are currently to acquire an adequate signal at all times. We present a proposal for improving AMT acquisition involving continuous profiling of the telluric field only during the daytime and AMT acquisition at a few base stations through the night.

INTRODUCTION

Natural-source time-varying electromagnetic (EM) waves observable on the surface of the Earth are generated by distant lightning activity at high frequencies (above about 1 Hz) and generally by the interaction of the Earth's magnetosphere with particles ejected by the Sun (solar plasma) at low frequencies (<1 Hz). These waves propagate around the globe in the electrically charged Earth–ionosphere waveguide, and they penetrate the Earth and respond, in both amplitude and phase, to the subsurface electrical conductivity structure. The frequency-domain transfer function relationship between the horizontal electric and magnetic field components measured on the surface of the Earth forms a 2×2 complex tensor, $\mathbf{Z}(\omega)$, which can be interpreted in terms of ground structure to depths given by the inductive scale length at the frequencies of interest. This geophysical technique, proposed independently yet simultaneously in the early 1950s in Russia (Tikhonov, 1950) and France (Cagniard, 1953) and now developed to be a highly advanced geological mapping tool, is called the magnetotelluric (MT) method (e.g., Vozoff, 1986, and references therein).

The high-frequency MT method, called audiomagnetotellurics (AMT), has recently seen widespread application for problems related to imaging the conductivity structure within the accessible part of the crust, i.e., the top 3 km. In Canada over the last few years, there have been more than 12 000 AMT soundings made for mineral exploration purposes, mostly around Voisey's Bay (Labrador), Sudbury (Ontario), and the Thompson nickel belt (Manitoba), particularly for regional mapping and for imaging structures at depths deeper than traditionally mined (>500 m) (e.g., Balch et al., 1998; Stevens and McNeice, 1998; Zhang et al., 1998). Controlled-source EM methods, used effectively in the past (Boldy, 1981), have their limitations for probing depths > ~500 m, and the AMT method offers greater depth penetration as well as a number of other attractive features: easier logistics, more tractable mathematical solutions for multidimensional targets, and the availability of 2-D and 3-D modeling and inversion codes.

However, critical to the successful application of AMT is the acquisition of high-quality time series data, which require sufficient natural signals during acquisition; the prior difficulties of the AMT method for shallow exploration were documented by Strangway et al. (1973). As a response, the controlled-source AMT method (CSAMT) was developed in the early 1970s (Goldstein and Strangway, 1975) because the sensors and instrumentation of the day could not detect the weak natural signals. Since that time there have been advances in sensors, instrumentation, and time-series processing schemes, such that

Manuscript received by the Editor February 23, 2000; revised manuscript received August 10, 2001.
*Formerly Geological Survey of Canada, 615 Booth Street, Ottawa, Ontario K1A 0E9, Canada; presently Woods Hole Oceanographic Institution, Deep Submergence Laboratory, Department of Applied Ocean Physics and Engineering, MS 9, Woods Hole, Massachusetts 02543. E-mail: xgarcia@whoi.edu.
‡Geological Survey of Canada, 615 Booth St., Ottawa, Ontario K1A 0E9, Canada. E-mail: ajones@nrcan.gc.ca.

at most AMT frequencies there is usually sufficient signal at all times of the day and for all seasons to ensure estimation of high-quality AMT transfer functions. However, a problem still exists in the so-called AMT dead band, of 1–5 kHz, where the natural signal spectrum exhibits lower amplitude. This is unfortunate because for typical hard-rock mining-scale problems in which a conducting mineralized body lies at 500 to 1500 m within a resistive host medium, it is precisely in this band of frequencies that the presence of the body is first sensed. Although the effects of the body are seen at lower frequencies (1 kHz–10 Hz), the body's parameters, geometry, and internal conductivity can only be determined optimally when its response is known over the full bandwidth. For the typical orebody discovered in Canada by EM methods up to the early 1980s (Boldy, 1981), the MT phases show maximum sensitivity to the body at two peaks: 2 kHz and 50 Hz. (The difference between the phases for a uniform host half-space and the phases for a space containing an anomalous body of enhanced conductivity is greatest at those frequencies.) The latter phase peak can be detected easily, but the former lies directly within the AMT dead band. The problem of the spectral minimum at these dead-band frequencies is exacerbated by diurnal, seasonal, and solar-cycle variations in signal amplitude levels. For example, as a consequence of the Earth's rotation, the atmosphere has a diurnal change in its ionic charge composition, affecting its conductivity and thus the attenuation of the EM waves that pass through it. There is also a seasonal variation caused by a decrease in the number of thunderstorms during the winter in the northern hemisphere and the summer in the southern hemisphere. Finally, solar output varies with the 11-year Chapman solar cycle, and this causes an 11-year cycle in atmospheric conductivity.

This paper examines the diurnal and seasonal variations in the AMT signal amplitude levels, with particular focus on the dead-band frequencies, and proposes an alternative strategy for acquiring AMT data. We first review the literature on the relevant physics of EM wave propagation through the atmosphere and describe the reasons for the diurnal and seasonal variation. We then analyze continuous AMT time series recorded in Canada and northern Germany to test the theories and to assess whether the AMT magnetic and electric sensors can record signals at all times or whether the typical signal amplitudes fall below sensor noise thresholds during certain times of the day or certain times of the year. With this information, we propose an optimized hybrid telluric-MT acquisition strategy given typical signal levels.

REVIEW OF ATMOSPHERIC PHYSICS

Let's review briefly the physics of the particle interaction in the Earth's atmosphere. Good general references are Tascione (1994), Ratcliffe (1972), Sentman (1985), Kelley (1989), and Davies (1990).

Physical properties of the atmosphere

The Sun's EM radiation contains short-wavelength energy that causes appreciable photoionization of the Earth's magnetosphere at high altitudes, resulting in a partially ionized region known as the ionosphere. This ionospheric region has a lower limit of 50 to 70 km above the Earth's surface but no distinct upper limit, although 2000 km is usually set arbitrarily as the upper limit for most purposes. The space between the surface of the Earth and the ionosphere forms a cavity or waveguide which can support EM standing waves with wavelengths comparable to planetary dimensions.

The vertical structure of the ionosphere changes continuously. It varies from day to night, with the seasons of the year, and with latitude. Furthermore, it is sensitive to enhanced periods of short-wavelength solar radiation accompanying solar (sunspot) activity, exhibiting a solar-cycle dependency. The ionosphere is categorized into a series of layers called, in order of increasing altitude and increasing electron concentration, D (90 km), E (110 km), F1 (200 km), and F2 (300 km). Electron density is greatest in the F2 region and decreases monotonically upward out to several Earth radii.

Diurnal variation is caused by the Earth's axial rotation. The sunlit side experiences ionization caused by solar photons. At night, the ions and electrons recombine. During the night the D region and the distinction between the two daytime F regions (F1 and F2) disappears. Also, there is a marked decrease in the maximum electron densities in the E and F2 regions by one to two orders of magnitude. Coupled with this diurnal variation is a seasonal variation. The daytime ionizations in the E and F1 regions are larger in summer than in winter, but the reverse is often true in the F2 region, a condition called the F2 seasonal anomaly. Finally, there is a long-period variation related to the 11-year sunspot cycle: at sunspot minimum, the electron densities are lower by a factor or two to four than at sunspot maximum, especially in the F region.

Diurnal and seasonal variations

In the 1920s, the *Carnegie* research vessel scientists observed the surface potential gradient over the oceans and measured the mean potential gradient at the surface of the Earth. This is known as the Carnegie curve (Figure 1a). The Carnegie curve suggests that the average variation of the surface potential gradient over the world's oceans has a maximum at 1830 universal time (UT) and a minimum at 0230 UT (Whipple, 1929; Markson, 1986). Watkins et al. (1998) analyzed and modeled a 25-year record of 10-kHz sferics noise in Antarctica and observed a diurnal variation with a minimum at 13 UT and a maximum at 23 UT. Chapman et al. (1966), studying the phase-velocity propagation in the Earth–ionosphere waveguide, obtained dispersion curves for day and night measurements and showed an increase of the dispersion curve and of attenuation during the daytime.

Sferics are EM pulses radiated by thunderstorms (Grandt, 1991). They are generated by large impulsive currents in the lightning channels, and they propagate through the Earth–ionosphere cavity. In a global study of sferics, different observatories worldwide measured pulses and calculated a distribution for different regions (Grandt, 1991). In the southern hemisphere, the main thunderstorm activity remains constant throughout the year; the maximum varies from winter to spring, but the minimum is generally observed in August (Figure 1b). An extensive study of the annual variation of EM waves is found in Chrissan and Fraser-Smith (1996).

The magnetic amplitude spectra over the frequency range 10^{-5}–10^{5} Hz was observed in Antarctica in June 1986 by Lanzerotti et al. (1990). The magnetic amplitude spectrum decreases with increasing frequency, f, as f^{-1} to $f^{-1.5}$. Recent observations by Farrel and Desch (1992) of the rare cloud-to-stratosphere lightning discharges (sprites and jets) suggest

that these events are inherently slow rising, with the emitted energy reaching peak values in about 10 ms. The authors show that emitted radio-wave energy from these events is strongest <50 Hz and possesses a significant rolloff at higher frequencies. In the ELF-VLF band the spectra level off at 10^3 Hz and increase again at $\sim 5 \times 10^3$ Hz. This decrease in the spectrum is largely a propagation effect related to a cut-off in the Earth–ionosphere waveguide. Lanzerotti et al. (1990) also show the 3-hour variation of the magnetic spectra. They did not see any appreciable difference between the night and day amplitudes for the ELF-VLF band, but the amplitude was larger for the daytime relative to the nighttime signal in the ULF band. One should remember that these studies were undertaken in June 1986 in the Antarctic—the beginning of the Austral winter when there is permanent night. The maximum ground current and electric field also occur over Antarctica (Hays and Roble, 1979).

DIURNAL AND SEASONAL VARIATIONS OF AMT TIME-SERIES SPECTRA

There are few published reports on studies of the variations of ionosphere EM waves and their direct bearing on AMT sounding. Jones and Argyle (1995) analyzed two days of data during which 40 Mb of high-frequency AMT signals, sampled at 25077.55 samples/s from six channels (H_x, H_y, remote H_x, remote H_y, E_x, E_y; where H denotes a magnetic channel, E an electric channel, and x and y denote north and east, respectively), were recorded for 140 s at the beginning of every hour. The estimated spectral amplitudes derived for the north-directed horizontal magnetic field component (H_x) at 1500 Hz frequency are illustrated in Figure 2. Jones and Argyle concluded that the highest activity levels at AMT deadband frequencies occurred in the evening and early morning hours (19:00 to 04:00) local time and decreased for the sunlight hours (08:00 to 16:00). Brasse and Rath (1997) studied source effects on AMT time series from northern Sudan and southern Egypt, analyzing the position of the source and the different features they associated with the Schumann resonances ($f = 7.8$ Hz, 14.1 Hz, 20.3 Hz, and higher-order harmonics). They demonstrated that although the major thunderstorm activity occurred in the late afternoon hours, the highest S/N ratio was in the nighttime—especially around local midnight.

To advance our understanding of diurnal and seasonal variations of signal amplitude, we analyzed two different time series: a large data set recorded over many months from Canada and a smaller set of a few days from northern Germany. The large data set comprised AMT time-series data recorded from May to October 1998 in the Sudbury area, northern Ontario (Canada). Each day, recording began at around 17:00 (local time) and continued through the night until around noon of the next day. The acquisition sequence consisted of recording 2048 samples at different frequency sample rates (6250, 6144, 3072, 384, and 48 Hz) sequentially. The northern German data set was comprised of almost continuous high-data-rate sampling at two sites during two days in January 1999.

Sudbury data set

To obtain robust spectral information from both of these data sets, we first applied orthogonal prolate spheroidal tapers to the data in the time domain and then used a fast Fourier transform algorithm (Chave et al., 1987). Subsequently, we processed all available data and compiled a sonogram for each of the four AMT components (H_x, H_y, E_x, E_y), with the power

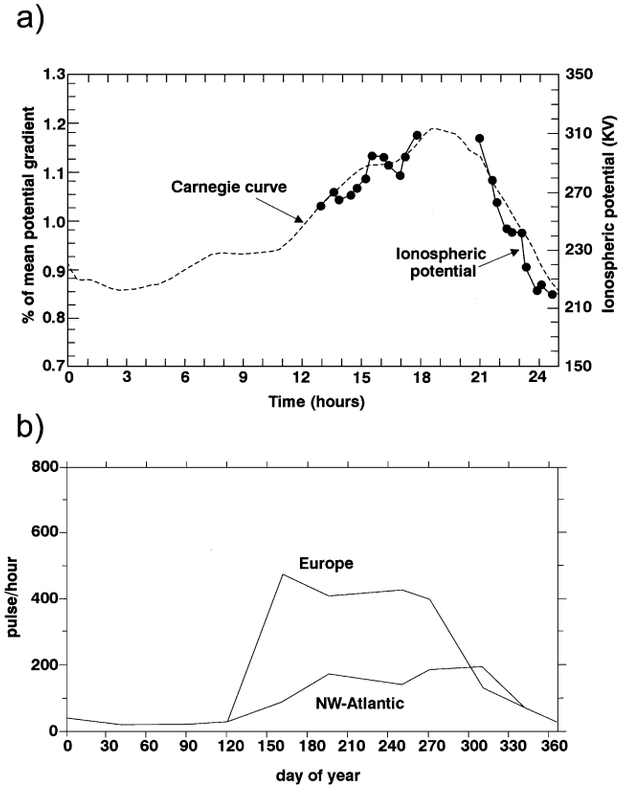

FIG. 1. The Carnegie curve, representing normalized surface potential gradient variations over the oceans in unperturbed conditions and measurements of ionospheric potential on September 7, 1984 (Markson, 1986). From Price (1993). (b) Annual sferic activity over Europe and the northwestern part of the Atlantic Ocean, recorded during 1989 and 1990. Reproduced from Grandt (1991).

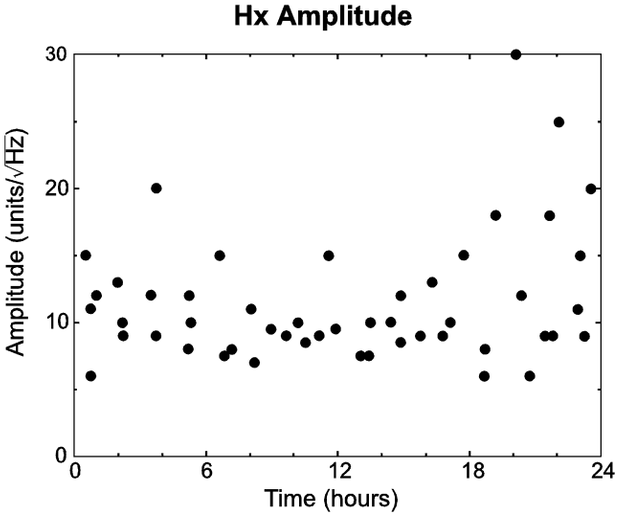

FIG. 2. Signal amplitude at 1500 Hz for different segments of data covering a day (arbitrary units). Note the weak levels during sunlight hours compared with the stronger levels at night. Reproduced from Jones and Argyle (1995).

spectra levels plotted against time of day and day of year. The plots for the H_x component at frequencies of 1000 and 2000 Hz are shown in Figures 3 and 4, respectively. The plots reconfirm that the highest signal levels occur at night, peaking at around local midnight. The power spectra differences between nighttime and daytime sections are up to four orders of magnitude, which equates to two orders of magnitude in signal amplitude. Another feature observed in the sonograms is an increase in signal amplitude over the whole day for the summer months compared to the spring months (May and early June). This is related to the seasonal variation in weather conditions that result in seasonal dependency in lightning storm activity, as pointed out by Price (1993), Sátori and Zieger (1996), Füllekrug and Fraser-Smith (1997), and Watkins et al. (1998). The power spectra at local midnight (Figure 5) also shows a seasonal dependence, although offset from the general daily trend because the signal is stronger at the beginning of summer (late June) than in the spring and fall. This maximum is consistent with the maximum in sferic activity in the northern hemisphere for the summer (Figure 1b).

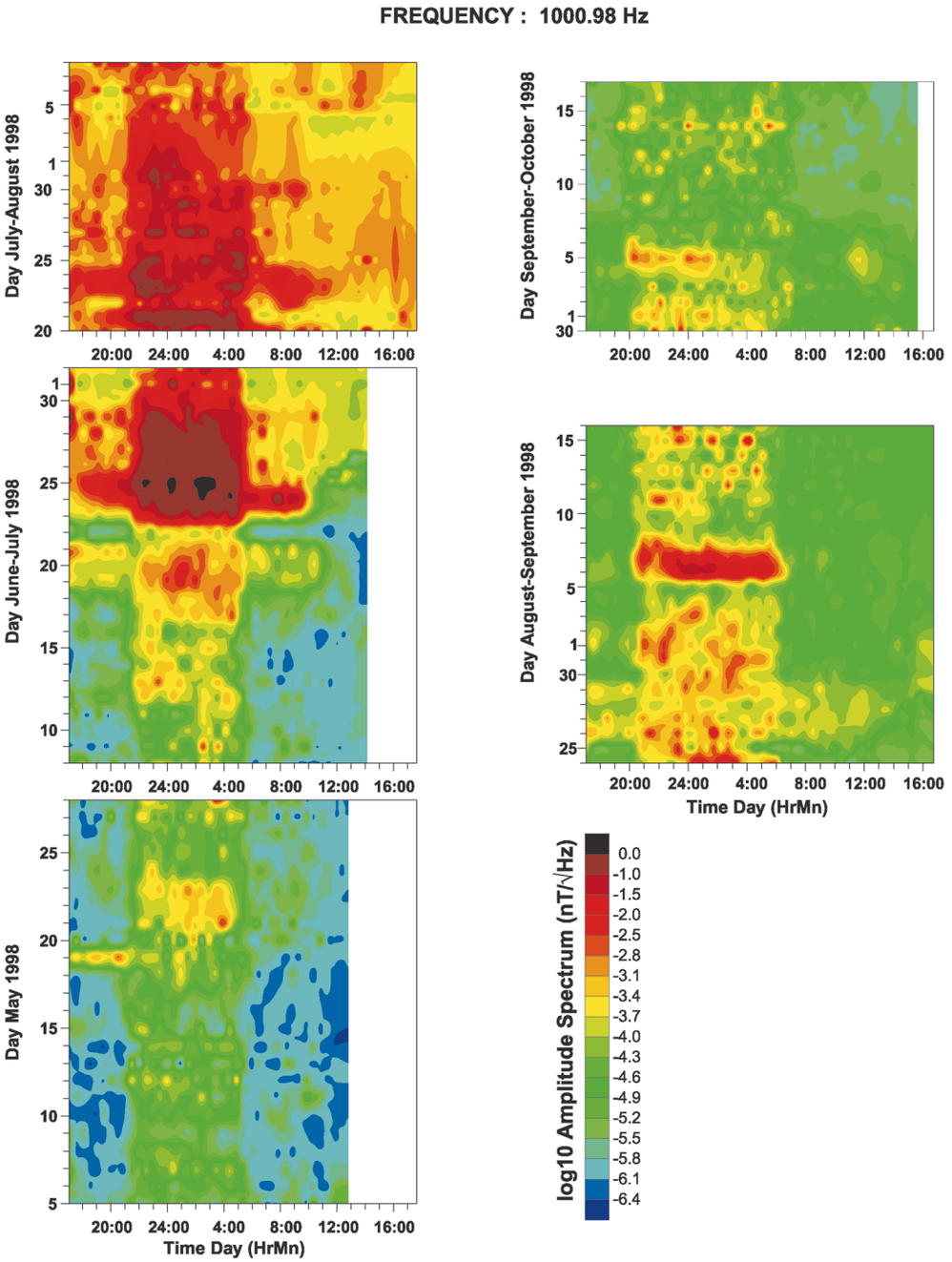

FIG. 3. Spectrograms corresponding to the H_x magnetic component calculated at 1000.98 Hz. Note the stronger signal around midnight and the higher activity by the end of June compared with the late spring and early fall months.

An example of the rapid attenuation in AMT dead-band signal amplitude at the onset of sunrise is shown in Figure 6. Note the amplitude spectra at 1000 Hz for all four components, covering almost 24 hours of recording between September 3 and 4, 1998. Sunrise was at 05:50 local time for this location, and the spectral amplitude drops precipitously at almost exactly that time.

Early September corresponds to the worst time for data acquisition at this location; the daylight hours are long, and the seasonal variation is at a minimum. Thus, an analysis of data from these days can provide information on whether it is possible to record dead-band AMT data under all conditions. The amplitude spectra of the magnetic fields in Figure 6 shows that after about 6 a.m. local time, i.e., sunrise, the time-series amplitude level (apart from sporadic intervals) is at the noise level of the induction coils, which is about 3×10^{-6} nT/$\sqrt{\text{Hz}}$, implying that the signal is below the coil noise threshold. To verify this result, an analysis of time series from three different time

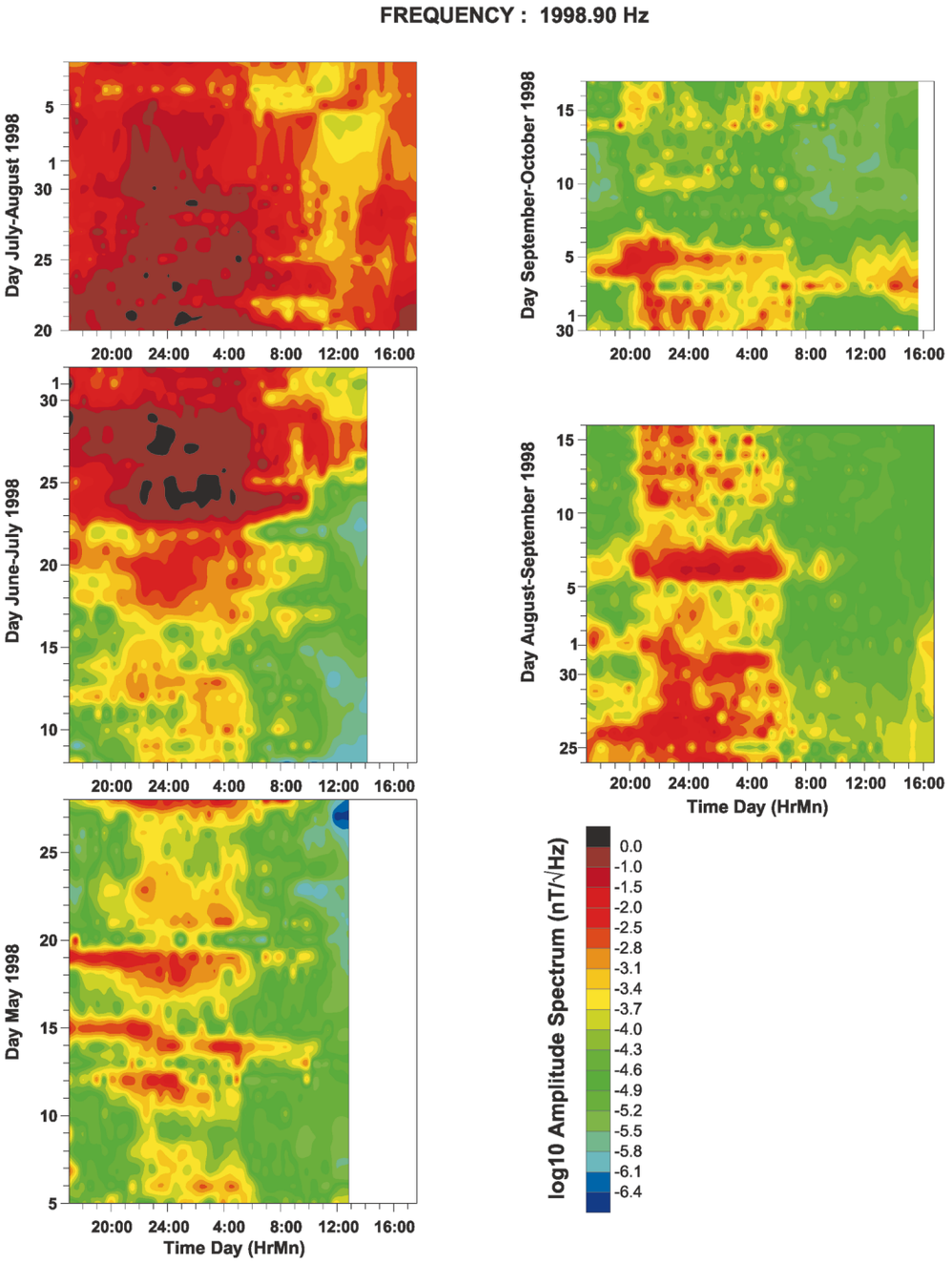

FIG. 4. Same as Figure 2 for a frequency of 1998.90 Hz. Note the stronger signal around midnight and the higher activity at the end of June compared with the late spring and early fall months.

intervals was performed (Figure 7). The first time series (dashed line) was recorded at 00:01:02 local time on September 4. Around the frequencies of interest, 1000–3000 Hz, there is good signal well above the coil noise level. The second time series (thick gray line) was recorded at 07:55:02 local time later that day. A comparison with the early time series shows a decay in signal amplitude of an order of magnitude at 1000 Hz. The thin black line shows the spectra corresponding to the time series recorded a few hours later (11:01:02). The signal amplitude decrease is clearly apparent, and the magnetic field spectra appear to be constant for frequencies >500 Hz, suggesting that the signal is below the noise level of the recording system. In contrast, however, the electric field spectra suggest that it is possible to record electric field AMT signals at any time of the day or night and during any season.

Northern Germany data set

To test whether these observations are a function of local time rather than location, we analyzed continuous AMT data recorded over 48 hours during January 1999 at two stations in northern Germany. The time series were acquired by Geosystem Srl. using induction coils built by Electro Magnetic Instruments Inc. (EMI). The diurnal amplitude spectral variation at 1000 and 2000 Hz for the four components from both sites are shown in Figures 8 and 9. The H_y spectral amplitudes at 1000 Hz show diurnal variation, with larger amplitudes during the nighttime—especially around local midnight—compared to the daytime. However, H_x amplitudes do not rise above the noise level of the induction coils at any time; thus, no reliable AMT estimates can be obtained for those frequencies at any time of the day or night. Although this result agrees with the seasonal dependence (Figure 9) representing the winter minimum, the lack of more data from the area does not permit us to determine if this is the result of a minimum in the annual variation. Note also, though, that the electric field amplitude spectra are reasonable, implying that AMT electric fields can be recorded with high quality at all times.

COIL SENSITIVITY

From the comparison of the magnetic and electric field spectral amplitudes during a 24-hour period, we can derive the maximum coil noise levels to ensure acquisition during relatively quiet intervals. Figure 6 shows H_x and H_y amplitude spectra at midnight of approximately 10^{-3} nT/$\sqrt{\text{Hz}}$, during which time the electric field amplitude levels are at approximately 10^4 mV/km/$\sqrt{\text{Hz}}$. This corresponds to a half-space of resistivity 2000 ohm-m (given by $\rho = 0.2 \times (E/H)^2/f$). During the daytime the electric field amplitude spectra drops to about 0.5 mV/km/$\sqrt{\text{Hz}}$, which would have an associated magnetic field signal amplitude level of 5.10^{-8} nT/$\sqrt{\text{Hz}}$. This signal level is two orders of magnitude below the best AMT coils currently available. To ensure signal acquisition during the daytime, far more sensitive magnetometers must be designed.

TELLURIC-MAGNETOTELLURIC (T-MT) ACQUISITION

An alternative approach to conventional four-component AMT data acquisition is to focus on telluric-only data acquisition during the day at as many locations as possible, with one or two sites being defined as base telluric sites. Then one could acquire AMT data through the night at the base telluric stations only. From the daytime data one can determine the site-telluric-to-base-telluric response functions; from the nighttime data, the base-MT response function. By multiplying these two transfer functions, one obtains the site-telluric-to-base-magnetic MT (M_bT) response for each site. Anomalous horizontal magnetic fields are usually small over conducting inhomogeneities, compared with the normal horizontal magnetic fields away from the inhomogeneities. Thus, provided the base station is reasonably close to the site although this is not the true MT response for that site as the distant base magnetic variations have been used instead of the (unrecorded) local site magnetic variations, there will be little difference between the M_bT response and the MT response. In addition, when undertaking 2-D inversion or 3-D modeling and/or inversion, one

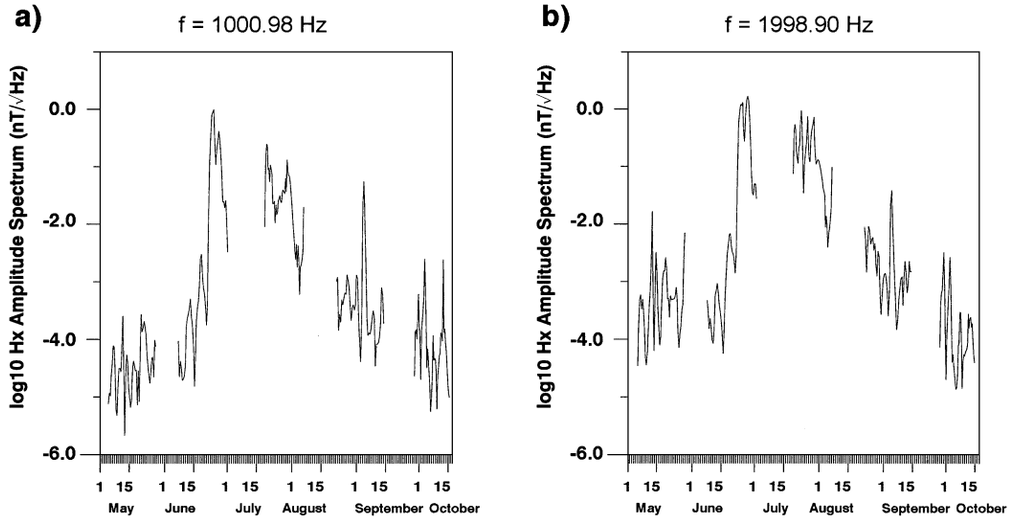

FIG. 5. Power spectra of the magnetic component H_x recorded at 00:00 local time for all the records available. Frequency is (a) 1000.98 Hz and (b) 1998.90 Hz.

can correctly relate the local model electric field to the distant base magnetic field to construct the model response function for comparison with the observed one.

This telluric-magnetotelluric AMT approach has the advantages of permitting acquisition during the day, when crews can efficiently and safely lay out equipment for 5 to 10 minutes acquisition then move to the next location. Also given the low cost of electrodes compared to magnetic field sensors, it is possible to undertake continuous field acquisition with (50-m) short dipoles. Such continuous tensor telluric profiling was first used across the Leitrim fault outside Ottawa in 1984 (reported in Poll et al., 1988) and has been advocated by Morrison and Nichols (1996). It is far superior to the EMAP technique (Torres-Verdin and Bostock, 1992), which involves in-line, along-profile electric field measurements only, given the insensitivity of such electric fields to subvertical conductors (see Jones, 1993). The MT acquisition at one or two base sites can be undertaken automatically. Indeed, for a small survey the same base sites could be used, requiring only MT acquisition over one night.

CONCLUSIONS

Natural signals traveling in the Earth–ionosphere resonant cavity experience attenuation resulting from atmospheric

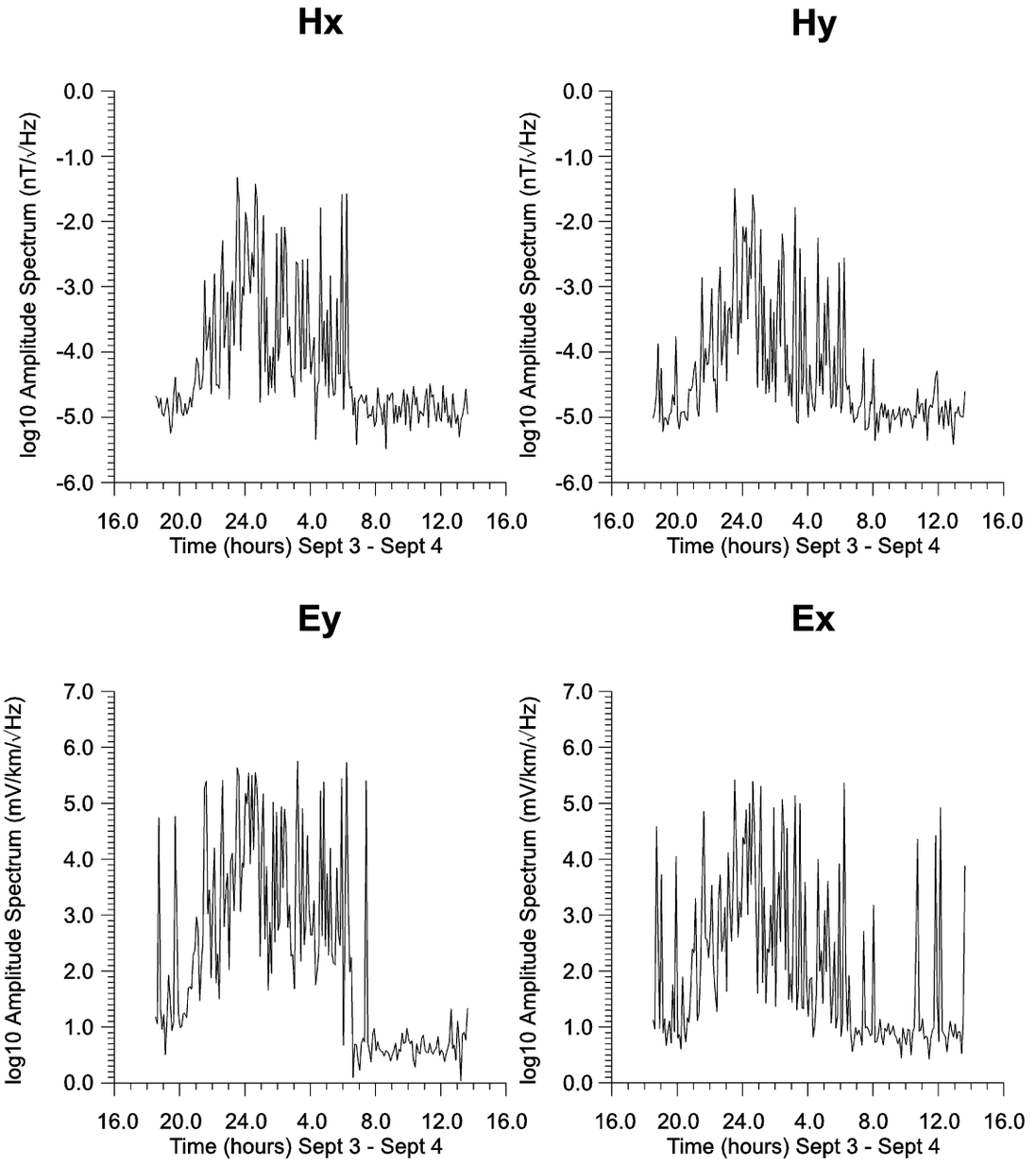

FIG. 6. Power spectra amplitude calculated for a frequency of 1000 Hz for the four electromagnetic channels recorded between the afternoon of September 3 and the morning of September 4. This time period corresponds to a minimum in the activity, as shown in Figure 3. Here, the difference is clear between the amplitude for the nightly hours compared with the daylight hours.

ionization from solar photons. This ionization exhibits a diurnal behavior because of the Earth's rotation, resulting in much higher atmospheric conductivity during the sunlit hours compared to the unlit (nighttime) hours. Thus, although the atmospheric electric field is larger during the day, it is much more strongly attenuated. We have shown that this diurnal variation likely occurs over the whole year, and also that there is a strong seasonal variation as a consequence of the seasonal variation in global lightning activity.

Our analyses show that often the magnetic field signal levels are below the coil noise threshold during the day, especially in the AMT dead band of 1 to 5 kHz. In contrast, nighttime signal levels are usually strong enough to provide good estimates of the transfer functions at AMT dead-band frequencies. The main conclusion that can be extracted from our study is that, for the frequency range used in the AMT method, the best time of the day to perform a sounding is during nighttime hours. The highest observable signal occurs when the whole propagation

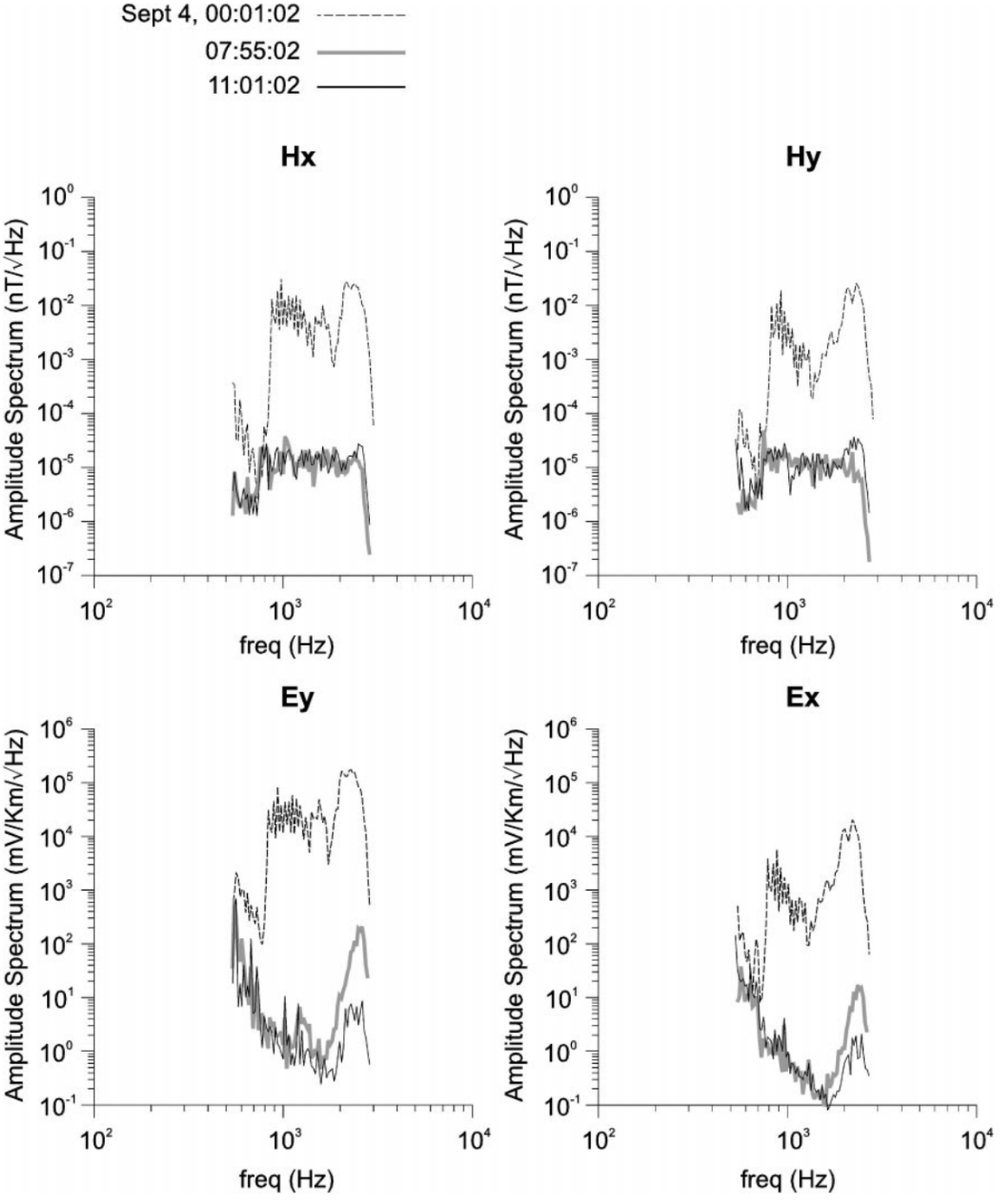

FIG. 7. Power spectra amplitude for three specific periods of time. A comparison of the three plots shows the decrease of the activity during the daytime hours compared to the midnight spectra. This particular day was considered to have the lowest activity (Figure 3).

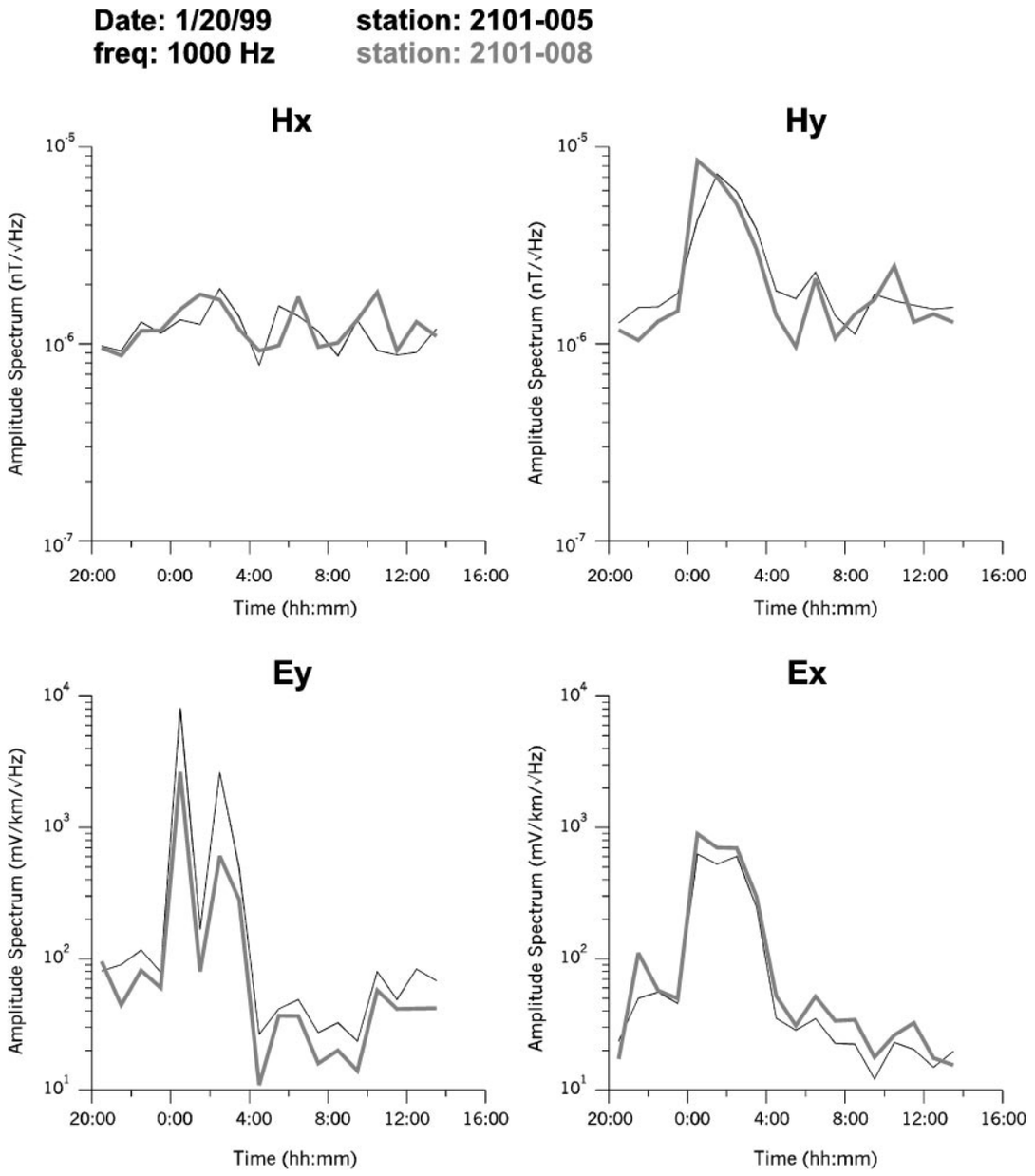

FIG. 8. Amplitude spectra correspondent to AMT data recorded in northern Germany during January 1999. The plot shows the four horizontal channels. The magnetic field amplitude spectra are very low, especially for the H_x channel. The H_y reading seems to improve during the nighttime, but it is close to the coil noise level (10^{-6} nT/$\sqrt{\text{Hz}}$). Spectra are calculated at 1000 Hz frequency for stations 2101-005 and 2101-008.

path from the lightning storm center to the site is unlit, which typically happens well into the night and explains the observed maximum at local midnight.

ACKNOWLEDGMENTS

The authors thank Gary McNeice of Phoenix Geophysics (Scarborough, Ontario, Canada) and Don Watts of Geosystem Srl. (Milan, Italy) for providing the AMT data used in this study and Kevin Stevens of Falconbridge Ltd. for permission to analyze the Sudbury data. Spectral amplitude estimates were obtained using the robust processing code of Alan Chave. Helpful and insightful comments by R. J. Banks, an anonymous reviewer, and associate editor M. Everett are also appreciated. X.G. is supported by an NSERC Research Fellowship funded by the Geological Survey of Canada (GSC), Phoenix Geophysics and Geosystem. GSC contribution 1999270.

REFERENCES

Balch, S., Crebs, T. J., King, A., and Verbiski, M., 1998, Geophysics of the Voisey's Bay Ni-Cu-Co deposits: 68th Ann. Internat. Mtg., Soc. Expl. Geophys., Expanded Abstracts, 784–787.

Boldy, J., 1981, Prospecting for deep volcanogenic ore: Can. Inst. Mining Bull., **74**, 55–65.

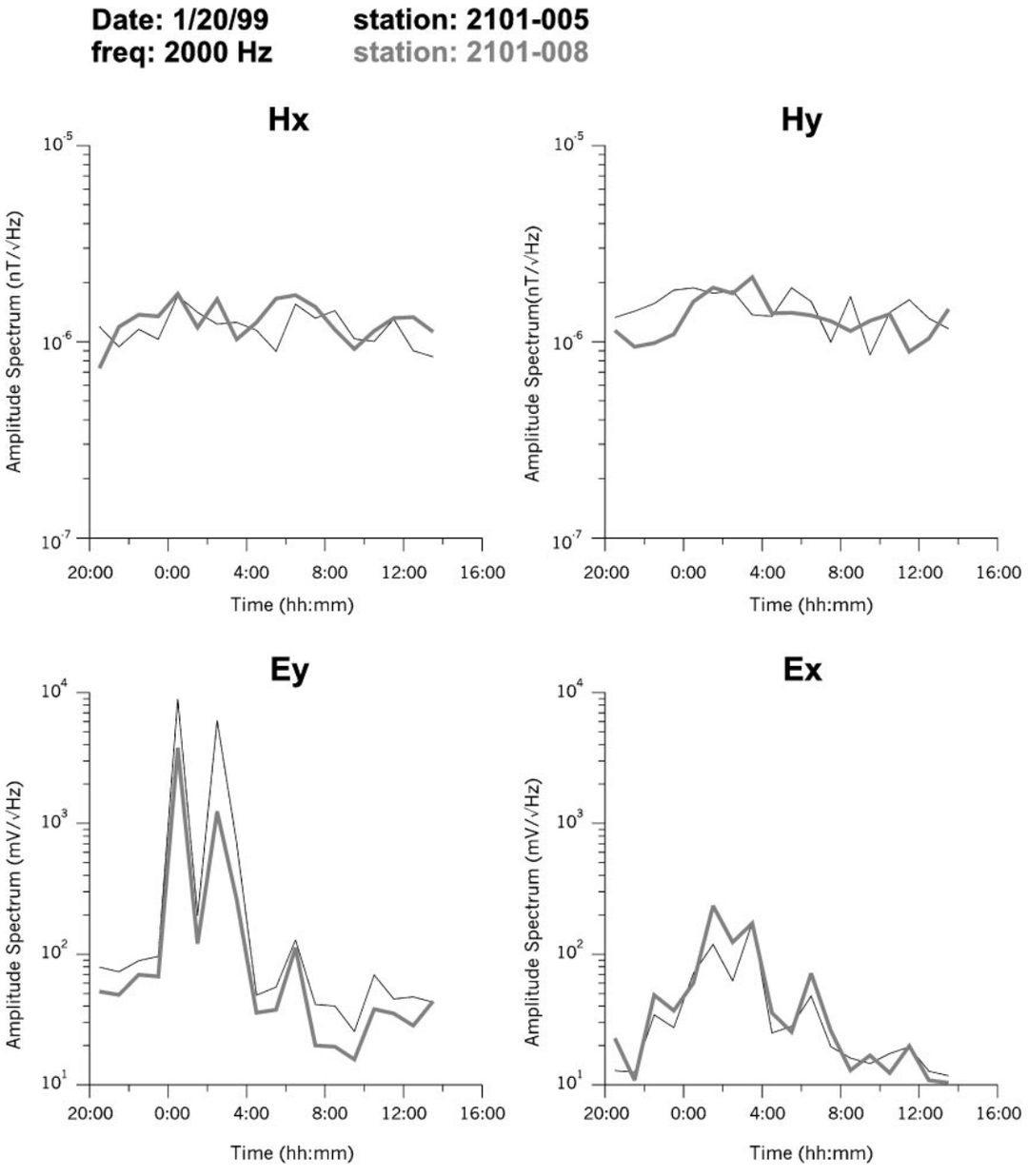

FIG. 9. Same as Figure 8, with amplitude spectra calculated at a frequency of 2000 Hz for station 2101-005 and 2101-008.

Brasse, H., and Rath, V., 1997, Audiomagnetotelluric investigations of shallow sedimentary basins in northern Sudan: Geophys. J. Internat., **128**, 301–314.

Cagniard, L., 1953, Basic theory of the magneto-telluric method if geophysical prospecting: Geophys., **18**, 605–635.

Chapman, F. W., Llanwyn Jones, D., Todd, J. D. W., and Challinor, R. A., 1966, Observations on the propagation constant of the earth-ionosphere waveguide in the frequency band 8 c/s to 16 kc/s: Radio Science, **1**, 1273–1282.

Chave, A. D., Thomson, D. J., and Ander, M. E., 1987, On the robust estimation of power spectra, coherences and transfer functions: J. Geophys. Res., **92**, 633–648.

Chrissan, D. A., and Fraser-Smith, A. C., 1996, Seasonal variations of globally-measured ELF/VLF radio noise: Radio Science, **31**, 1141–1152.

Davies, K., 1990, Ionospheric radio: Peter Peregrinus Ltd.

Farrell, W. M., and Desch, M. D., 1992, Clouds-to-stratosphere lightning discharges: A radio emission model: Geophys. Res. Lett., **19**, 665–668.

Füllekrug, M., and Fraser-Smith, A. C., 1997, Global lightning and climate variability inferred from ELF magnetic field variations: Geophys. Res. Lett., **24**, 2411–2414.

Goldstein, M. A., and Strangway, D. W., 1975, Audio-frequency magnetotellurics with a grounded electric dipole source: Geophysics, **40**, 669–683.

Grandt, C., 1991, Global thunderstorm monitoring by using the ionospheric propagation of VLF lightning pulses (sferics) with applications to climatology: Ph.D. thesis, University of Bonn.

Hays, P. B., and Roble, R. G., 1979, A quasi-static model of global atmospheric electricity, **1**—The lower atmosphere: J. Geophys. Res., **84**, 3291–3305.

Jones, A. G., 1993, The COPROD2 dataset: Tectonic setting, recorded MT data and comparison of models: J. Geomag. Geoelectr., **45**, 933–955.

Jones, A. G., and Argyle, M., 1995, Display and processing of high frequency magnetotelluric data: Geological Survey of Canada Report of 1994/1995 Industrial Partners Program activities.

Kelley, M. C., 1989, The earth's ionosphere: Academic Press.

Lanzerotti, L. J., Maclennan, C. G., and Fraser-Smith, A. C., 1990, Background magnetic spectra: Geophys. Res. Lett., **96**, 15973–15984.
Markson, R., 1986, Tropical convection, ionospheric potentials, and global circuit variation: Nature, **320**, 588–594.
Morrison, H. F., and Nichols, E. A., 1996, Continuous impedance profiling for mineral exploration: 66th Ann. Internat. Mtg., Soc. Expl. Geophys., Expanded Abstracts, 1286–1289.
Poll, H., Weaver, J. T., and Jones, A. G., 1988, Calculations of voltages for magnetotelluric modelling of a region with near-surface inhomogeneities: Phys. Earth Planet. Int., **53**, 287–297.
Price, C., 1993, Global surface temperatures and the atmospheric electrical circuit: Geophys. Res. Lett., **20**, 1363–1366.
Ratcliffe, J. A., 1972, An introduction to the ionosphere and magnetosphere: Cambridge Univ. Press.
Sátori, G., and Zieger, B., 1996, Spectral characteristics of Schumann resonances observed in central Europe: J. Geophys. Res., **101**, 29663–29669.
Sentman, D. D., 1985, Schumann resonances, *in* Volland, H., Ed., CRC handbook of atmospheric electrodynamics: CRC Press.
Stevens, K. M., and McNeice, G., 1998, On the detection of Ni-Cu ore hosting structures in the Sudbury Igneous Complex using the magnetotelluric method: 68th Ann. Internat. Mtg., Soc. Expl. Geophys., Expanded Abstracts, 751–755.
Strangway, D. W., Swift, C. M., and Holmer, R. C., 1973, The application of audio frequency magnetotellurics (AMT) to mineral exploration: Geophysics, **38**, 1159–1175.
Tascione, T. F., 1994, Introduction to the space environment: Krieger Publ. Co.
Tikhonov, A. N., 1950, On the determination of hte electric characteristics of deep layers of the earth's crust: Dolk. Acad. Nauk. SSSR, **73**, 295–297.
Torres-Verdin, C., and Bostick, F. X., 1992, Principles of spatial surface electric field filtering in magnetotellurics: Electromagnetic array profiling (EMAP): Geophysics, **57**, 603–622.
Vozoff, K., Ed., 1986, Magnetotelluric methods: Soc. Expl. Geophys. Reprint Series 5.
Watkins, N. W., Clilverd, M. A., Smith, A. J., and Yearby, K. H., 1998, A 25-year record of 10 kHz noise in Antarctica: Implications for tropical lightning levels: Geophys. Res. Lett, **25**, 4353–4356.
Whipple, F. J. W., 1929, On the association of the diurnal variation of electric potential gradient in fine weather with the distributions of thunderstorms over the globe: Quart. J. Roy. Met. Soc., **55**, 1–17.
Zhang, P., King, A., and Watts, D., 1998, Using magnetotellurics for mineral exploration: 68th Ann. Internat. Mtg., Soc. Expl. Geophys., Expanded Abstracts, 776–779.